Analysis of a Bent Slot Antenna with a Parasitic Element for Dual Band Operation

Takehiro MORIOKA, Kazuhiro HIRASAWA and Satoshi SHIBASAKI

Institute of Information Sciences and Electronics, University of Tsukuba
Tsukuba, Ibaraki, Japan305

1. Introduction

We propose a bent slot antenna with a parasitic wire element for dual band operation at 825 MHz and 1430 MHz. Antenna characteristic such as VSWR. radiation pattern ,magnetic current on the slot and electric current on the parasitic element are calculated by the method of moments. Calculated VSWR is in good agreement with the measured data. We found that the slot was resonated at 825 MHz and the parasitic element became resonant at 1430 MHz.

2. Antenna Structure

A bent slot antennas is made on an infinite ground plane and a parasitic wire is set over the slot as shown in fig. 1. The two ends of the parasitic wire are connected to the ground plane. The lengths of the slot and the parasitic wire are adjusted to a half wavelength at a higher frequency and a lower frequency, respectively, for dual band operation. The feed point on the slot is located near the end A and is fed by a coaxial cable. The parasitic wire from point F to K is parallel and the EF and KL are vertical to the ground plane. It is assumed that the height of the parasitic wire is 8 mm, the wire diameter is 0.9 mm and the slot width is 1 mm.

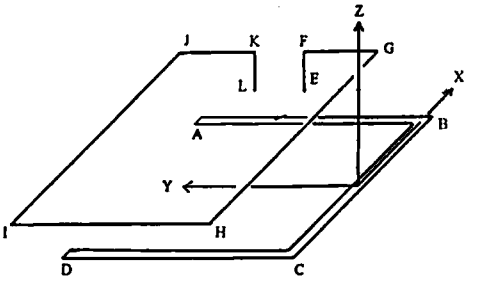

fig.1 Antenna structure

3. Numerical Results

Since the slot width is narrow, a thin magnetic current is assumed on the slot and image theory is used to remove the ground plane. The magnetic current on the slot and the electric current on the parasitic wire are obtained by the method of moments.

3.1 VSWR

The calculated and measured VSWR are shown in fig. 2. In this paper a resonance frequency is defined as the frequency for the minimum VSWR. This figure shows that the antenna has two resonant frequencies at 825 MHz and 1430

MHz. At the lower resonance the calculated and measured bandwidths (VSWR ≤ 2) are 7 MHz and 10 MHz, respectively. The bandwidth may be increased by using a thicker parasitic wire.

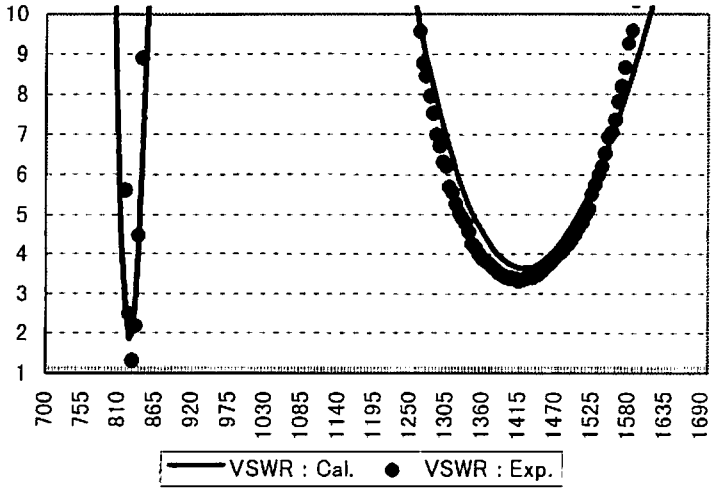

fig.2 VSWR

3.2 Magnetic and Electric Current

The amplitude of the magnetic current on the slot and that of the electric current on the parasitic wire at 825 MHz are shown in fig. 3a and b. At 825 MHz the parasitic wire is about a half wavelength and the electric current becomes dominant. The electric current on the parasitic wire becomes zero and changes the phase midway between points H and I. Figs. 4a and b show the magnetic current on the slot and the electric current on the parasitic wire at 1430 MHz. The slot length becomes about a half wavelength and the slot is resonated. And the amplitude of the magnetic current becomes much larger compared with the one at 825 MHz.

3.3 Radiation Pattern

Fig. 5 shows the calculated radiation pattern. At 825 MHz the radiation from the parasitic wire is larger compared with the one from the slot. In the X-Z plane E_ϕ at 825 MHz is much smaller than that at 1430 MHz. In the Y-Z plane E_θ at 825 MHz has a null in the $\theta = 0°$ direction. The reason is that the large electric currents flow from G to F and from J to K, but their contribution to E_θ in the $\theta = 0°$ direction is canceled. At 1430 MHz the radiation from the slot is dominant. Thus in the Y-Z plane E_θ is the radiation from the slot B C and becomes omnidirectional. In the X-Z plane the radiation from the slot is zero in the $\theta = 0°$ direction ,but the radiation from the parasitic wire fills the null.

4. Conclusion

We analyzed the bent slot antenna with a parasitic wire for dual band operation. The calculated VSWR agrees well with the measured data. We found that from the calculated current distribution the slot radiation was strong at 1430 MHz and

the radiation from the parasitic wire was dominant at 825 MHz. To increase the bandwidth at the lower resonance and to lower the VSWR at the higher resonance are underway.

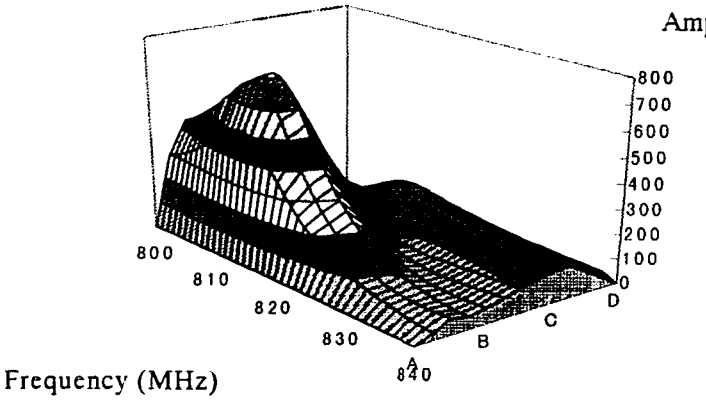

fig.3a Magnetic current distribution

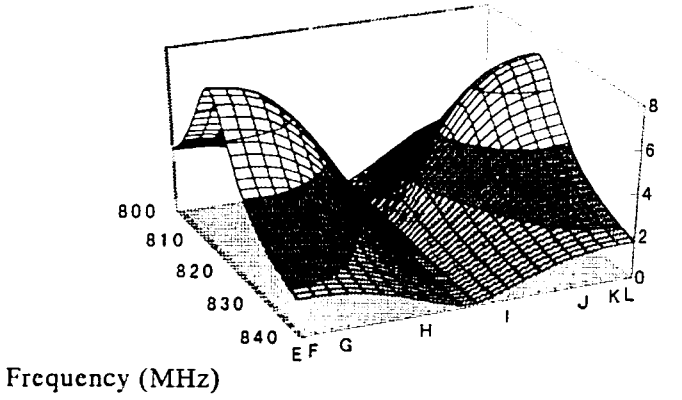

fig.3b Electric current distribution

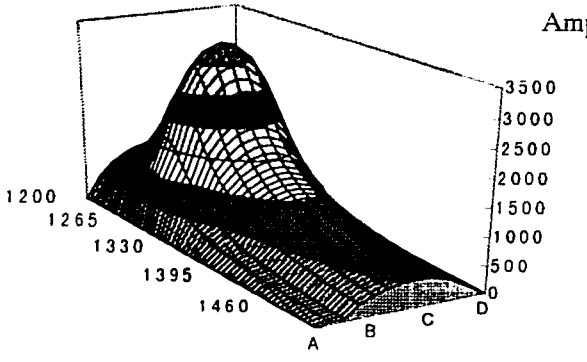

fig.4a Magnetic current distribution

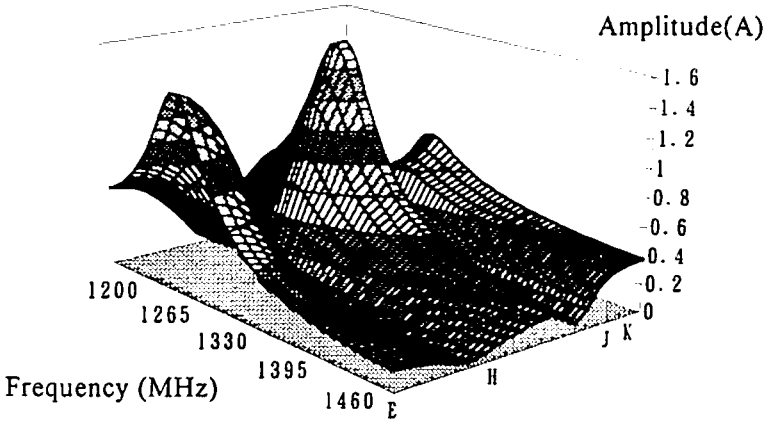

fig.4b Electric current distribution

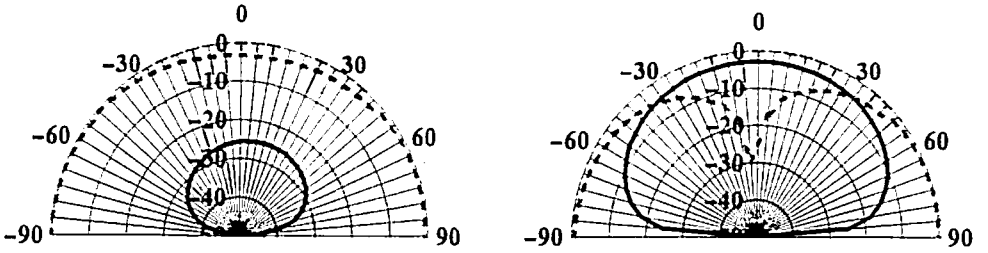

fig.5a Radiation pattern

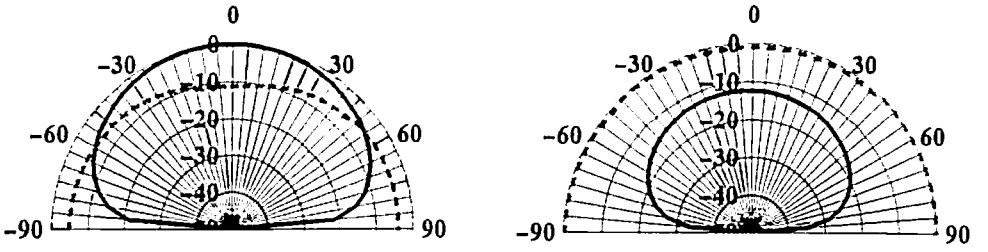

fig.5b Radiation pattern